*Supporting Information for*

# NMR-Derived Models of Amidopyrine and its Metabolites Complexed to Rabbit Cytochrome P450 2B4 Reveal a Structural Mechanism of Sequential *N*-Dealkylation[†]

*Arthur G. Roberts*[a,d], *Sara E. A. Sjögren*[b], *Nadezda Fomina*[a], *Kathy T. Vu*[c], *Adah Almutairi*[a], *James R. Halpert*[a]

[a]University of California, San Diego, The Skaggs School of Pharmacy and Pharmaceutical Sciences, 9500 Gilman Drive #0703, La Jolla, CA 92093-0703. [b]Lund University, BMC F12, S-221 84 Lund, Sweden.[c]University of Gothenburg, Sahlgrenska Academy, Box 400, 405 30 Gothenburg, Sweden.

Email: a1roberts@ucsd.edu

RUNNING TITLE: Structural Mechanism of Sequential *N*-Dealkylation

[d] Correspondence should be addressed to the University of California, San Diego, The Skaggs School of Pharmacy and Pharmaceutical Sciences, 9500 Gilman Drive #0703, La Jolla, CA 92093-0703. Telephone: (858) 822-7804. Fax (858) 246-0089. [†] This study was supported by National Institute of Health (NIH) grant ES003619.

**Results**

*Simulation of $r_{app}$, $r_{avg}$ and $R_P$.* To better understand the effect of time averaging on the $r_{app}$, $r_{avg}$ and $R_P$, a simulation of a proton on a phenyl molecule was performed. In the simulation the phenyl proton approaches within 6 Å ($r_{close}$) of the heme iron. When the phenyl group flips with the orientation of the proton opposite to the heme, the maximum distance will be 5 Å greater or a total distance of 11 Å ($r_{far}$). In this simulation, the molecule can only be in two positions; close and far. After mathematical manipulation of eq 6, $r_{app}$ becomes:

$$r_{app} = \sqrt[6]{\frac{r_{close}^6 r_{far}^6}{f_{close} r_{far}^6 + f_{far} r_{close}^6}} \qquad \text{(S1)}$$

When $r_{far} > r_{close}$, eq S1 can be simplified to:

$$r_{app} \cong \sqrt[6]{\frac{r_{close}^6}{f_{close}}} \qquad \text{(S2)}$$

where $f_{close}$ and $f_{far}$ are the fraction of time in the close and far positions, respectively. The apparent distance ($r_{app}$) is different than the time-averaged distance $r_{avg}$, when $f_{far} > 0$ :

$$r_{avg} = f_{close} r_{close} + f_{far} r_{far} \qquad \text{(S3)}$$

Subsequently, $R_P$ has similar time averaging behavior as $r_{avg}$, when $f_{far} > 0$:

$$R_p = f_{close} R_{close} + f_{far} R_{far} \qquad \text{(S4)}$$

$$R_p \cong f_{close} R_{close} \qquad \text{(S5)}$$

where $R_{close}$ and $R_{far}$ are the close and far relaxation rates, respectively. For this simulation, the $R_{close}$ was arbitrarily set to 2 $s^{-1}$, which would make $R_{far}$ based on distances equal to 0.053 $sec^{-1}$ (i.e. $(11^{-6}/6^{-6})*2$).

Figure S1 shows the simulation of $r_{app}$, $r_{avg}$ and $R_P$ using the Equations S1, S3 and S4 and the effect of $r_{app}$ and $r_{avg}$, when the molecule spends a certain fraction of the time close to the heme. When the molecule is oriented with the proton close to the heme 15% of the time (i.e. $f_{close} = 0.15$), the $r_{app}$ is 8 Å, while the $r_{avg}$ is 10.25 Å. When the proton is in this oriented 50% of the time in the closer position, the $r_{app}$ is reduced to 6.7 Å compared with an $r_{avg}$ of 8.5 Å. When the simulated proton spends even a small amount of time at the closer distance, the calculated $r_{app}$ is skewed toward the shorter distance (Figure S1A). The skewing effect helps explain why distances calculated with the Solomon-Bloembergen equation in a number of studies are not as dispersed as one might expect, such as those found by Regal and Nelson (1). In Figure S1, the equation for $R_P$ is plotted with respect to the fraction of time in the closer ($f_{close}$) orientation. The trend of $R_P$ is linear with respect to $f_{close}$, which resembles the trend of $r_{avg}$, except that the slope has the opposite sign. In other words, smaller $r_{avg}$ is going to have a higher $R_P$ and a larger $r_{avg}$ is going to have a lower $R_P$.

This linear relationship does not mean that it is possible to calculate $r_{avg}$ from $R_P$, because the magnitudes of the slopes cannot be correlated. The linearity simply means that the time averaging of known $R_P$ rates and known distances is similar. Because of the $r^6$ distance and linear relationship of $r_{app}$ and $R_P$, respectively, $R_P$ is considerably more sensitive to orientation than $r_{app}$. In cases were the molecule is highly mobile, $R_P$ may provide a better sense of the preferred orientation than $r_{app}$. On the other hand, if molecules are only in a single orientation (i.e. $f_{far} = 0$), then $r_{app}$ might also accurately represent the orientation because $r_{app}$ would then equal $r_{avg}$. Therefore, the relationship of $R_P$ and $r_{app}$ with respect to orientation should be treated carefully, but may be useful for understanding qualitatively the orientation and movement in the active site.

*NMR Peak Shifts of AP and its Metabolites Show that They are in Fast Exchange.* P450 ligands exchange between the P450 active site and the solvent. At high ligand to protein ratios, the interaction between drugs and P450 is examined indirectly by probing drugs in the bulk solvent. This requires that drugs exchange on the order of hundreds of microseconds, or faster.

Fast exchange of drug binding is usually determined by examining the temperature-dependence of the $R_P$ (*1-5*). However, these experiments are complicated by two factors. First, the spin state of P450s is temperature sensitive (*6-9*). Second, if the $K_D$ is temperature-dependent, the drug may bind in a different orientations depending on the temperature. To avoid these problems, shifts and broadening of ligand NMR peaks can be monitored to determine if ligands are in fast exchange (*1*).

Since all the molecules bind to P450 2B4 with $K_D$'s in the mM range, these ligands were expected to be fast exchange. To test whether these ligands were indeed in fast exchange, the chemical shifts of the NMR peaks were examined in the presence of oxidized and reduced P450 2B4 as done previously (*1, 10*). As shown in Figure S2 there are clear shifts in the aromatic region of the DMAP NMR spectrum in the presence of oxidized vs. reduced P450 2B4. Similar shifts were observed for AP and AAP (data not shown). Thus, all the molecules were in fast exchange.

The effect of P450 2B4 on the relaxation of AP and its metabolites can also be diagnostic for fast exchange because intermediate and slowly exchanging ligands have distinct effects on the NMR spectra and the observed $R_P$s. First, the NMR linewidth of the ligand-bound NMR signal for a ligand in intermediate or slow exchange is broadened many fold (*11, 12*). Because the area of the ligand-bound NMR peak remains constant, the increase in linewidth leads to a decrease in amplitude of the NMR peak. In other words, the signal will essentially be absent from the NMR spectrum. Second, because of the long residence time of the ligand bound to the protein in these exchange regimes, the observed relaxation rate will no longer be a mixture of ligand-bound and –free relaxation rates. Instead, the observed relaxation rate of the prominent NMR ligand signal will relax at the same rate as a ligand that

is free in solution. Since the molecules were significantly relaxed by P450 2B4, they were all in fast exchange.

**References**


1. Cameron, M. D., Wen, B., Allen, K. E., Roberts, A. G., Schuman, J. T., Campbell, A. P., Kunze, K. L., and Nelson, S. D. (2005) Cooperative binding of midazolam with testosterone and α-naphthoflavone within the CYP3A4 active site: a NMR $T_1$ paramagnetic relaxation study, *Biochemistry 44*, 14143-14151.
2. Cameron, M. D., Wen, B., Roberts, A. G., Atkins, W. M., Campbell, A. P., and Nelson, S. D. (2007) Cooperative binding of acetaminophen and caffeine within the P450 3A4 active site, *Chem. Res. Toxicol. 20*, 1434-1441.
3. Hummel, M. A., Gannett, P. M., Aguilar, J. S., and Tracy, T. S. (2004) Effector-mediated alteration of substrate orientation in cytochrome P450 2C9, *Biochemistry 43*, 7207-7214.
4. Modi, S., Primrose, W. U., Boyle, J. M., Gibson, C. F., Lian, L. Y., and Roberts, G. C. (1995) NMR studies of substrate binding to cytochrome P450 BM3: comparisons to cytochrome P450 cam, *Biochemistry 34*, 8982-8988.
5. Regal, K. A., and Nelson, S. D. (2000) Orientation of caffeine within the active site of human cytochrome P450 1A2 based on NMR longitudinal ($T_1$) relaxation measurements, *Arch. Biochem. Biophys. 384*, 47-58.
6. Cinti, D. L., Sligar, S. G., Gibson, G. G., and Schenkman, J. B. (1979) Temperature-dependent spin equilibrium of microsomal and solubilized cytochrome P-450 from rat liver, *Biochemistry 18*, 36-42.
7. Fisher, M. T., and Sligar, S. G. (1987) Temperature jump relaxation kinetics of the P-$450_{cam}$ spin equilibrium, *Biochemistry 26*, 4797-4803.

8. Renaud, J. P., Davydov, D. R., Heirwegh, K. P., Mansuy, D., and Hui Bon Hoa, G. H. (1996) Thermodynamic studies of substrate binding and spin transitions in human cytochrome P-450 3A4 expressed in yeast microsomes, *Biochem. J. 319 ( Pt 3)*, 675-681.

9. Ristau, O., Rein, H., Greschner, S., Janig, G. R., and Ruckpaul, K. (1979) Quantitative analysis of the spin equilibrium of cytochrome P-450 LM2 fraction from rabbit liver microsomes, *Acta Biol. Med. Ger. 38*, 177-185.

10. Gay, S. C., Roberts, A. G., Maekawa, K., Talakad, J. C., Hong, W. X., Zhang, Q., Stout, C. D., and Halpert, J. R. (2010) Structures of cytochrome P450 2B4 complexed with the antiplatelet drugs ticlopidine and clopidogrel, *Biochemistry 49*, 8709-8720.

11. Levitt, M. H. (2001) *Spin Dynamics: Basics of Nuclear Magnetic Resonance*, John Wiley & Sons, LTD, New York.

12. Kowalewski, J., and Mäler, L. (2006) *Nuclear spin relaxation in liquids : theory, experiments, and applications*, Taylor & Francis, New York.

13. Oda, A., Yamaotsu, N., and Hirono, S. (2005) New AMBER force field parameters of heme iron for cytochrome P450s determined by quantum chemical calculations of simplified models, *J. Comput. Chem. 26*, 818-826.

14. Scott, E. E., White, M. A., He, Y. A., Johnson, E. F., Stout, C. D., and Halpert, J. R. (2004) Structure of mammalian cytochrome P450 2B4 complexed with 4-(4-chlorophenyl)imidazole at 1.9 Å resolution: Insight into the range of P450 conformations and coordination of redox partner binding, *J. Biol. Chem. 279*, 27294-27301.

15. Autenrieth, F., Tajkhorshid, E., Baudry, J., and Luthey-Schulten, Z. (2004) Classical force field parameters for the heme prosthetic group of cytochrome c, *J. Comput. Chem. 25*, 1613-1622.

**Table S1.** *Additional Force field parameters used for P450 2B4*[a]

| Bond | Energy (kcal $mol^{-1}$ $Å^{-2}$) | Distance (Å)[b] | Reference |
|---|---|---|---|
| Fe-S | 87.589 | 2.377 | (*13*) |

| Angle[c] | Energy (kcal $mol^{-1}rad^{-2}$) | Reference |
|---|---|---|
| Fe-S-$C_b$ | 21.646 | (*13*) |
| $N_P$-Fe-S | 13.277 | (*13*) |

| Dihedral[c] | Energy (kcal $mol^{-1}$) | Reference |
|---|---|---|
| $C_b$-S-Fe-$N_P$ | 0.034[d] | (*13*) |

[a] Fe, heme iron; S, sulfur of C435; $C_b$, $C_b$ of C435; $N_P$, pyrrole heme nitrogen.

[b] Equilibrium distance value from (*13*).

[c] The angles and dihedrals, used in the simulations, were calculated using the values measured from the P450 2B4 X-ray crystal structure (*14*).

[d] Autenrieth et al., 2004 obtained energy values for cytochrome c of 0.04 kcal $mol^{-1}$(*15*)

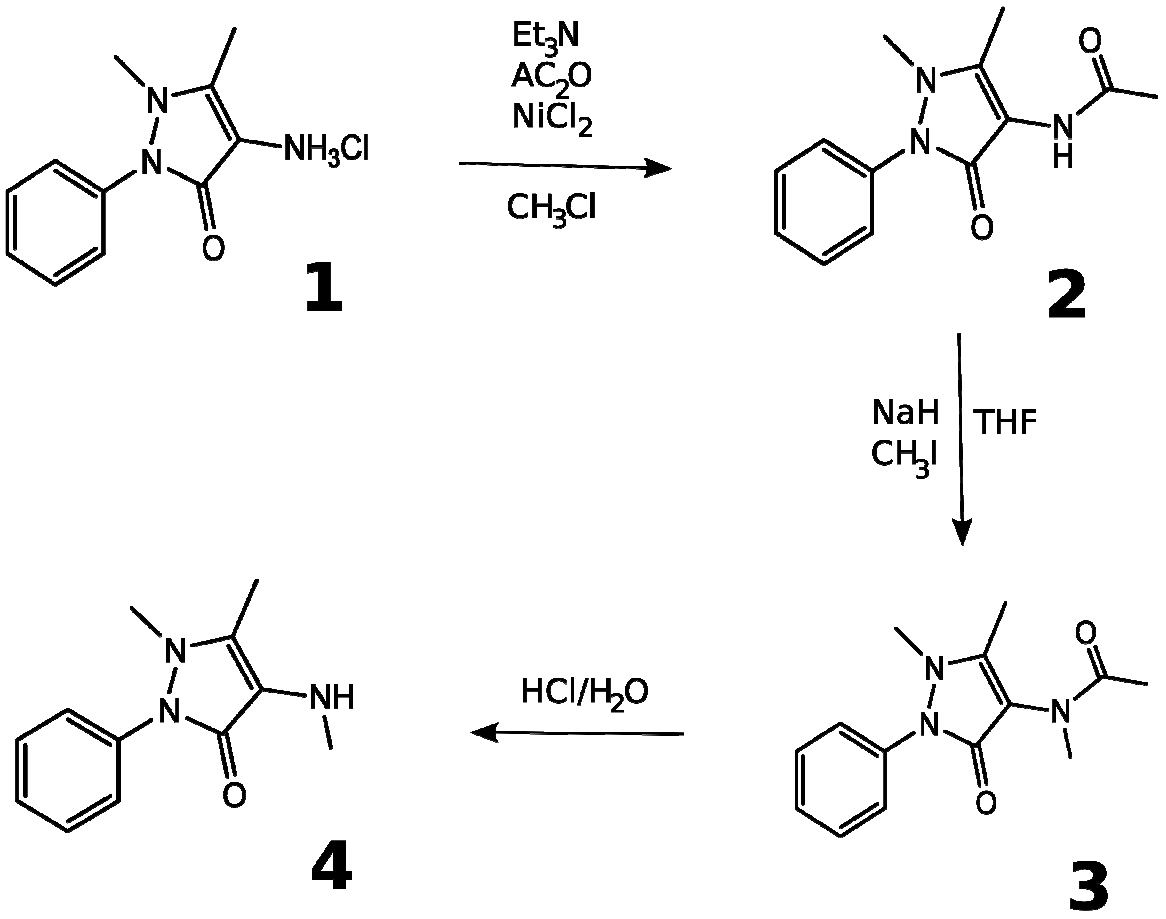


**Scheme S1.** Synthesis of DMAP.

**Figure Legends**

**Figure S1.** *The effect of time averaging on $r_{app}$, $r_{avg}$ and $R_P$.* A. Calculated $r_{app}$ (solid line) and $r_{avg}$ (dotted line). B. Paramagnetic relaxation ($R_P$) with respect to the fraction of time in the closer orientation (i.e. $f_{close}$).

**Figure S2.** *1D $^1$H NMR Spectrum of 1.0 mM DMAP in 99% D2O with 40 μM of oxidized (top) and reduced (bottom) with CO-reduced P450 2B4.* Only the peaks labeled 2'/6', 3'/5' and 4' of the aromatic region are shown. Vertical lines are put onto the graph to emphasize the shifts.

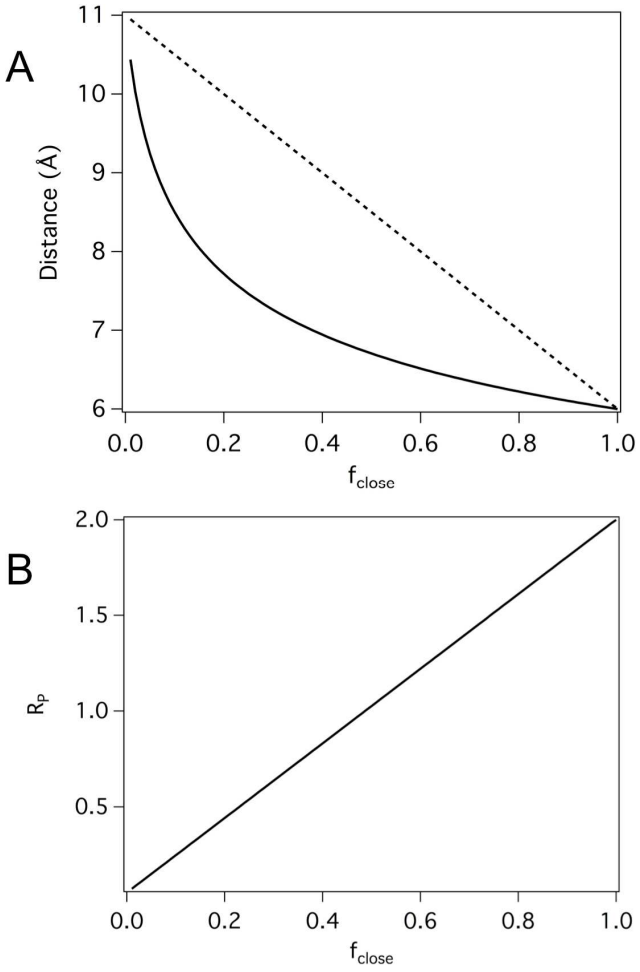
A
Distance (Å)
11
10
9
8
7
6
0.0
0.2
0.4
0.6
0.8
1.0
f close
B
R p
2.0
1.5
1.0
0.5
0.0
0.2
0.4
0.6
0.8
1.0
f close

**Figure S1.**

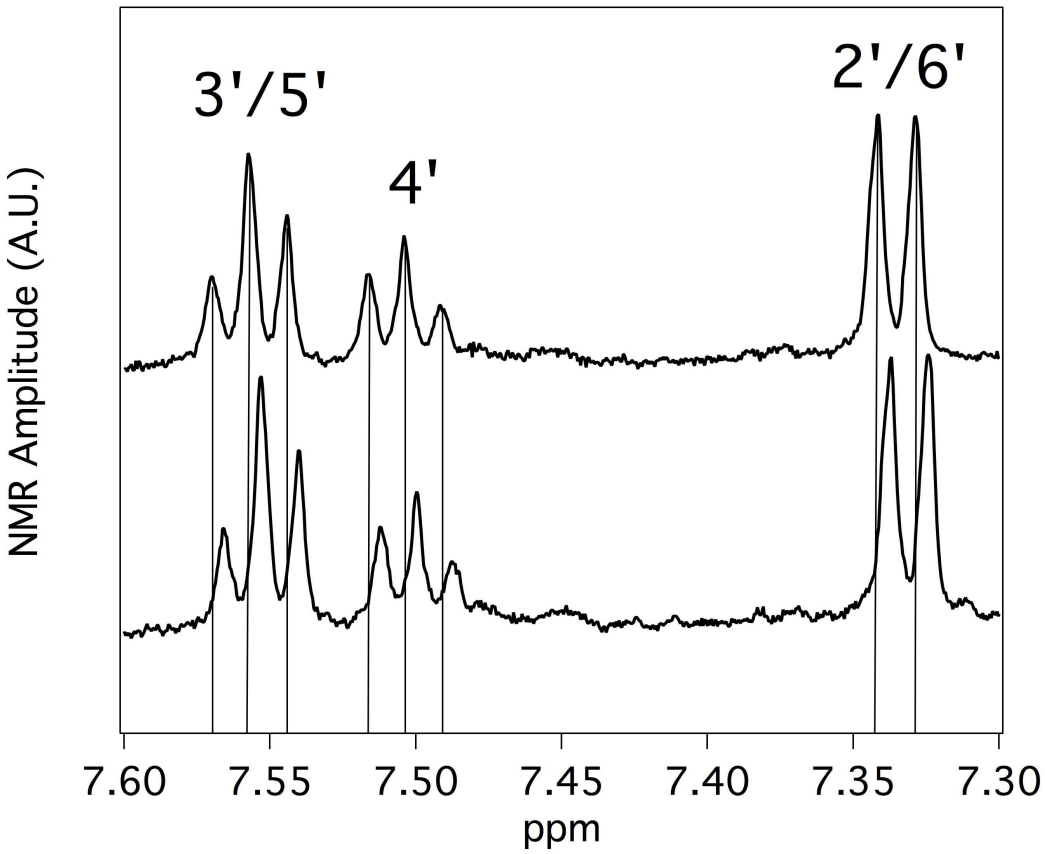


**Figure S2.**